Inorg. Chem. **2007**, *46*, 2575–2583

Conformational Flexibility in 2,2′-Dioxybiphenyl-chloro-cyclotetraphosphazenes and its Relevance to Polyphosphazene Analogues

Eric W. Ainscough,*,† Andrew M. Brodie,*,† Adrian B. Chaplin,‡ Andreas Derwahl,† John A. Harrison,§ and Carl A. Otter†

Chemistry—Institute of Fundamental Sciences, Massey University, Private Bag 11 222, Palmerston North, New Zealand, Institut des Sciences et Ingénierie Chimiques, Ecole Polytechnique Fédérale de Lausanne (EPFL), CH-1015 Lausanne, Switzerland, and Chemistry—Institute of Fundamental Sciences, Massey University, Private Bag 102 904, North Shore Mail Center, Auckland, New Zealand

Received November 10, 2006

The reaction of the cyclotetraphosphazene, $[N_4P_4Cl_8]$, with the difunctional reagent, 2,2′-biphenol, in the presence of potassium carbonate in acetone produced the spiro-substituted derivatives, 2,2′-dioxybiphenylhexachlorocyclotetraphosphazene, bis(2,2′-dioxybiphenyl)tetrachloro-cyclotetraphosphazene, and tris(2,2′-dioxybiphenyl)dichlorocyclotetraphosphazene. Both cis and trans geometrical isomers of the bis compound are observed. Although chromatographic separation of these was unsuccessful, a sample of the trans isomer was obtained by fractional crystallization. The compounds all show non-first-order ^{31}P NMR spectra which were simulated to extract the spectral parameters. Single-crystal X-ray structures of both the trans bis and the tris compounds show that the cyclophosphazene rings exhibit conformational flexibility which gives rise to different crystalline forms being obtained from the same solvent systems. Crystals of *trans*-bis(2,2′-dioxybiphenyl)tetrachloro-cyclotetraphosphazene were obtained in two different space groups: P*nna* (orthorhombic) and $P2_1/n$ (monoclinic). In the orthorhombic structure, the dominant (72%) conformation of one phosphazene ring is a chair form, and the other (28%) resembles a boat. While for the monoclinic structure, the ring is virtually flat with an oval shape. In both cases the dioxybiphenyl groups are found in R and S configurations in the same molecule and are π stacked in columns (*Pnna*) or involved in π–π or π–H interactions ($P2_1/n$), thus anchoring the phosphorus atoms of the cyclotetraphosphazenes but still allowing flexibility in the ring conformations. Three crystalline modifications of tris(2,2′-dioxybiphenyl)dichloro-cyclotetraphosphazene were obtained: two in space group $P\bar{1}$ (triclinic), which contained two molecules of dichloromethane in the unit cell, and one solvent-free form in space group $P2_1/n$ (monoclinic). The cyclophosphazene rings exhibit puckered conformations with the *trans*-dioxybiphenyl moieties having opposing RS or SR conformations. DFT calculations were carried out on each of the phosphazene ring conformations in *trans*-bis(2,2′-dioxybiphenyl)-tetrachlorocyclotetraphosphazene identified from the X-ray diffraction analysis. It is concluded that intermolecular interactions (i.e., π–π or π–H) between the dioxybiphenyl groups is a factor that modifies the nature of the potential energy surface between the different conformers. The flexibility of the phosphazene ring is supported computationally through the calculated low-energy barriers and experimentally through the highly disordered phosphazene ring conformations observed in the solid state. The results on 2,2′-dioxybiphenyl-substituted cyclotetraphosphazenes provide evidence that microcrystalline domains in their 2,2′-dioxybiphenyl-substituted polyphosphazene analogues will be generated by similar π–π and π–H interactions.

Introduction

Phosphazenes, particularly polyphosphazenes, continue to receive considerable commercial interest because of their diverse range of material properties. Appropriately substituted, polyphosphazenes have been employed as flame resistant materials, elastomers, membranes, solid ionic conductors, and inert biomaterials.[1] In addition, the rich substitution chemistry at the phosphorus center not only

* To whom correspondence should be addressed. E-mail: e.ainscough@massey.ac.nz (E.W.A.); a.brodie@massey.ac.nz (A.M.B.).
† Massey University, Palmerston North.
‡ Ecole Polytechnique Fédérale de Lausanne (EPFL).
§ Massey University, Auckland.

(1) Allcock, H. R. *Chemistry and Applications of Polyphosphazenes*; Wiley-Interscience: Hoboken, NJ, 2003.

10.1021/ic062141t CCC: $37.00
Published on Web 03/03/2007

Scheme 1

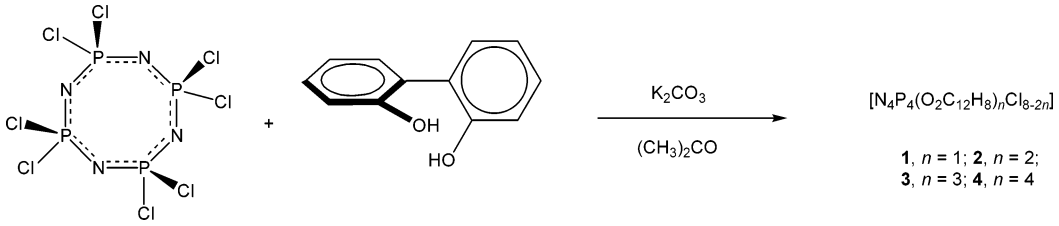

allows the manipulation of these and other material properties but also has the possibility for immobilization of catalytic or bioactive moieties.[1,2]

Cyclic or short-chain linear phosphazenes are valuable small molecule models for the polymeric systems, which are often difficult to characterize because of their higher molecular weight and structural complexity. Of these model systems, the cyclotriphosphazenes, $[N_3P_3R_6]$, are the most prevalent. Structural data for tetrameric systems are less common, although these and higher oligomers provide better structural analogues. This is primarily because of the flexible nature of the ring, which can assume a number of different conformations, whereas the cyclic trimers are generally planar. For example, in a series of cyclic trimers containing large or sterically demanding substituents reported by Allcock and co-workers, the PNP angle deviated little from around 122°, while this angle in corresponding tetramers varied between 121 and 157°.[3] In linear polyphosphazenes, the angle at the nitrogen is estimated to be in the range of 130−160°, and the low-energy barrier to this variation contributes significantly to the flexibility of the polymer backbone.[1]

Polyphosphazenes containing spirocyclic groups such as 2,2′-dioxybiphenyl and 2,2′-dioxynapthyl, recently reported by Carriedo and co-workers, have shown interesting properties.[4] For example, the fully substituted polymers are resistant to extreme chemical conditions and have some of the highest glass transition temperatures known for polyphosphazenes.[4a] The group have recently reported a stable polymer containing 2,2′-dioxybiphenyl, amino, and PCl groups (the later having remained unreacted from the chloropolymer precursor),[4b] which is remarkable given the hydrolytic susceptibility usually associated with the polymeric phosphazene P−Cl bond.

While a large variety of cyclotriphosphazene derivates containing aromatic spirocyclic groups are known,[5] including the homologous series of cyclotriphosphazenes incorporating mono-spiro, bis-spiro, and tris-spiro 2,2′-dioxybiphenyl substituents,[5a,b,g] there are few examples for the cyclic tetramers. In the case of the 2,2′-dioxybiphenyl substituent, only the tetrakis-spirocyclic derivative is known.[6] Hence, we have undertaken a study on cyclic phosphazene tetramers containing 2,2′-dioxybiphenyl groups to gain an insight into the interactions that may result from the loading of phosphazene polymers/oligomers with these functions. We have also performed DFT calculations to assess the contribution of the spirocyclic groups to the energy barriers that influence the flexibility of the phosphazene ring.

Hence, in this report, we describe the synthesis and characterization of partially substituted 2,2′-dioxybiphenylcyclotetraphosphazenes and find that because of the flexible nature of the tetrameric ring and concomitant interactions between the 2,2′-dioxybiphenyl substituents, these compounds are more appropriate model compounds for the corresponding partially substituted polyphosphazenes than the trimer analogues.[5a,f,7] The compounds are also useful precursors for preparing other models of mixed-substituent phosphazenes.

Results and Discussion

Syntheses. The reaction of 2,2′-biphenol with octachlorocyclotetraphosphazene, $[N_4P_4Cl_8]$, in acetone in the presence of excess K_2CO_3 gave mixtures composed of 2,2′-dioxybiphenylhexachloro-cyclotetraphosphazene (**1**), bis(2,2′-dioxybiphenyl)tetrachlorocyclotetraphosphazene (**2**), tris(2,2′-

(2) (a) Dubois, R. A.; Garrou, P. E.; Lavin, K. D.; Allcock, H. R. *Organometallics* **1986**, *5*, 460−466. (b) Pertici, P.; Vitulli, G.; Salvadori, P.; Pitzalis, E.; Gleria, M. *Phosphazenes* **2004**, 621−631. (c) Chandrasekhar, V.; Athimoolam, A. *Org. Lett.* **2002**, *4*, 2113−2116. (d) Chandrasekhar, V.; Athimoolam, A.; Srivatsan, S. G.; Sundaram, P. S.; Verma, S.; Steiner, A.; Zacchini, S.; Butcher, R. *Inorg. Chem.* **2002**, *41*, 5162−5173.

(3) (a) Allcock, H. R.; Al-Shali, S.; Ngo, D. C.; Visscher, K. B.; Parvez, M. *J. Chem. Soc., Dalton Trans.* **1996**, 3549−3559. (b) Allcock, H. R.; Al-Shali, S.; Ngo, D. C.; Visscher, K. B.; Parvez, M. *J. Chem. Soc., Dalton Trans.* **1995**, 3251−3532. (c) Allcock, H. R.; Ngo, D. C.; Parvez, M.; Visscher, K. *J. Chem. Soc., Dalton Trans.* **1992**, 1687−1699. (d) Ainscough, E. W.; Brodie, A. M.; Derwahl, A. *Polyhedron* **2003**, *22*, 189−197.

(4) (a) Carriedo, G. A.; García-Alonso, F. J. *Phosphazenes: A Worldwide Insight*; Gleria, M., de Jaeger, R., Eds.; Nova Science Publishers Inc.: New York, 2004; pp 171−190 and references therein. (b) Carriedo, G. A.; García-Alonso, F. J.; Pancorbo, D. L. *Eur. Polymer. J.* **2007**, *43*, 57−64.

(5) For examples, see: (a) Carriedo, G. A.; Fernández-Catuxo, L.; Garcia-Alonso, F. J.; Gómez-Elipe, P.; González, P. A. *Macromolecules* **1996**, *29*, 5320−5325. (b) Allcock, H. R.; Stein, M. T.; Stanko, J. A. *J. Am. Chem. Soc.* **1971**, *93*, 3173−3178. (c) Allcock, H. R.; Turner, M. L.; Visscher, K. B. *Inorg. Chem.* **1992**, *31*, 4354−4364. (d) Allcock, H. R.; Kugel, R. L. *Inorg. Chem.* **1966**, *5*, 1016−1020. (f) Dez, I.; Levalois-Mitjaville, J.; Grützmacher, H.; Gramlich, V.; de Jaeger, R. *Eur. J. Inorg. Chem.* **1999**, 1673−1684. (e) Brandt, K.; Porwolik-Czomperlik, I.; Siwy, M.; Kupka, T.; Shaw, R. A.; Davies, D. B.; Hursthouse, M. B.; Sykara, G. D. *J. Am. Chem. Soc.* **1997**, *119*, 12432−12440. (f) Kumaraswamy, S.; Vijjulatha, M.; Muthiah, C.; Swamy, K. C. K.; Engelhardt, U. *J. Chem. Soc., Dalton Trans.* **1999**, 891−899. (g) Carriedo, G. A.; Garcia-Alonso, F. J.; García-Alvarez, J. L.; Pappalardo, G. C.; Punzo, F.; Rossi, P. *Eur. J. Inorg. Chem.* **2003**, 2413−2418.

(6) Allcock, H. R.; Walsh, E. J. *Inorg. Chem.* **1971**, *10*, 1643−1647.

(7) (a) Marcelo, G.; Saiz, E.; Mendicuti, F.; Carriedo, G. A.; García-Alonso, F. J.; García-Alvarez, J. L. *Macromolecules* **2006**, *39*, 877−885. (b) Carriedo, G. A.; Crochet, P.; García-Alonso, F. J.; Gimeno, J.; Presa-Soto, A. *Eur. J. Inorg. Chem.* **2004**, 3668−3674. (c) Carriedo, G. A.; García-Alonso, F. J.; Valenzuela, C. D.; Valenzuela, M. L. *Polyhedron*, **2006**, *25*, 105−112. (d) Carriedo, G. A.; García-Alonso, F. J.; Presa, A. *J. Inorg. Organomet. Polymers* **2004**, *14*, 29−37.

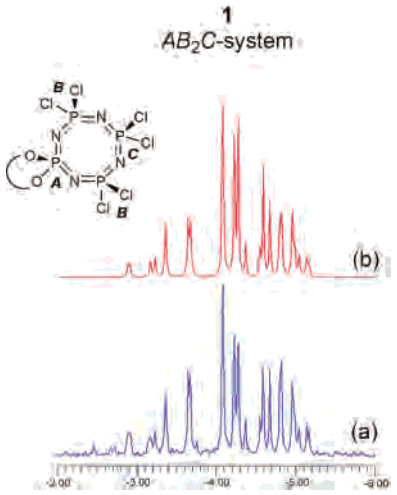

Figure 1. ^{31}P NMR spectrum for **1** with assignments: (a) observed spectrum and (b) simulated spectrum.

dioxybiphenyl)dichlorocyclotetraphosphazene (**3**), and tetrakis(2,2′-dioxybiphenyl)-cyclotetraphosphazene (**4**) as depicted in Scheme 1. Compound **1** is obtained in good yield (∼90%), using a 1:1 ratio, with only minor contamination of **2** (∼3−4%), which can be removed by recrystallization from CH_2Cl_2−hexane. This is comparable to the analogous 1:1 reaction with hexachlorocyclotriphosphazene, $[N_3P_3Cl_6]$, where the mono-spiro-substituted derivative is formed in an ∼91% yield containing ∼3% of the bis-spiro derivative.[5a] In a similar manner, compounds **2** (54% yield) and **3** (72% yield) were also obtained, using molar ratios of 2:1 and 3:1, respectively, although with lower selectivity and requiring chromatographic separation. Both cis and trans geometrical isomers of compound **2** are observed, although a small preference for the trans-substituted derivative is found (∼1.4:1 at 0 °C), presumably because of the increased steric hindrance of the 2,2′-dioxybiphenyl moiety to substitution at an adjacent center, even at an elevated temperature (∼1.3:1 at 56 °C). While chromatographic separation was unsuccessful, small portions of the trans isomer can be isolated by fractional crystallization.

^{31}P NMR Spectra. Since compounds **1**−**3** all show non-first-order ^{31}P NMR spectra, it was necessary to carry out simulation analysis to extract the appropriate spectral parameters. Following this analysis, we have assigned both **1** and **3** as AB_2C spin systems (Figures 1 and 3), and the corresponding parameters are listed in Table 1. In the case of **2**, two unique spin systems, corresponding to the different geometrical isomers, are observed (Figure 2) and unambiguously assigned by comparison to the spectra of pure *trans*-**2** which was obtained by fractional crystallization. The *cis*-**2** isomer shows two multiplets at δ 1.71 and −3.92 ppm which are assigned to an AA′BB′ spin system, whereas the resonances for the *trans*-**2** isomer are observed as a multiplet centered at $\delta \approx -2.8$ ppm matching an A_2B_2 spin system.

Single-Crystal X-ray Structures. X-ray diffraction analyses of both *trans*-**2** and **3** show that in the solid state the cyclotetraphosphazene rings exhibit conformational flexibility

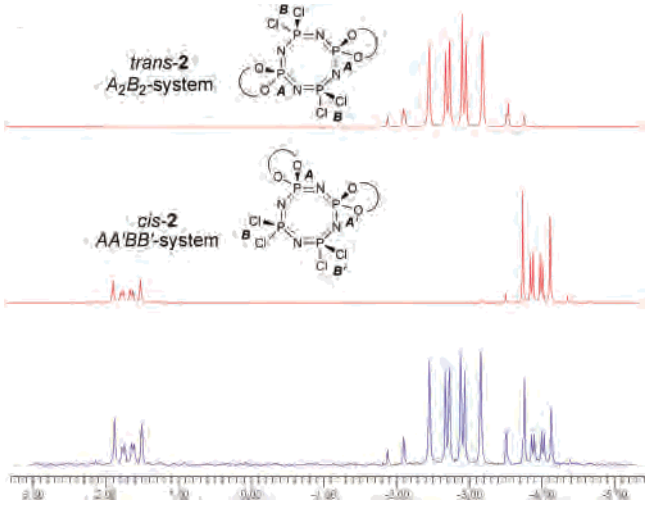

Figure 2. Simulated (above with assignments) and observed (below) ^{31}P NMR spectra for **2** (mixture of cis and trans isomers).

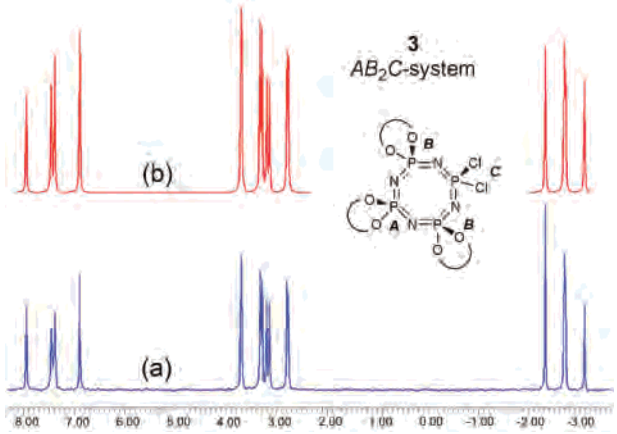

Figure 3. ^{31}P NMR spectrum for **3** with assignments: (a) observed spectrum and (b) simulated spectrum.

Table 1. ^{31}P NMR Spectroscopic Data for **1**, **2**, and **3**[a]

		δ (ppm)			J (Hz)		
	spin system	A/A$_2$/AA′	B$_2$/BB′	C	$J_{AA'}$	J_{AB}	$J_{BC}/J_{BB'}$
1	AB_2C	−3.37	−4.33	−4.96		65.0	29.2
trans-**2**	A_2B_2	−2.45	−3.18			64.7	
cis-**2**	AA′BB′	1.71	−3.92		29.0	60.8	84.6
3	AB_2C	7.38	3.24	−2.70		86.4	63.2

[a] Obtained from simulation analysis. Measured in $CDCl_3$ at 298 K.

and that different crystalline forms can arise from the same solvent system.

Hence, crystallization of **2** was achieved on two separate occasions from CH_2Cl_2−hexane, giving crystals of *trans*-**2** in two different space groups: P*nna* (orthorhombic) (*trans*-**2*A***) and $P2_1/n$ (monoclinic) (*trans*-**2*B***). The orthorhombic structure, *trans*-**2*A***, exhibits molecules that have a highly disordered phosphazene ring conformation (Figure 4). The disordered portion of the structure was satisfactorily refined into three parts, containing two different phosphazene ring conformations. The dominant (72%) conformation (*trans*-**2*Aa*** and *trans*-**2*Ab***, Figure 4) resembles a chair form, with the P2 phosphorus centers deviating (0.7 Å) above and below a plane defined by the remaining ring centers. The minor conformation (*trans*-**2*Ac***) is more twisted and resembles a

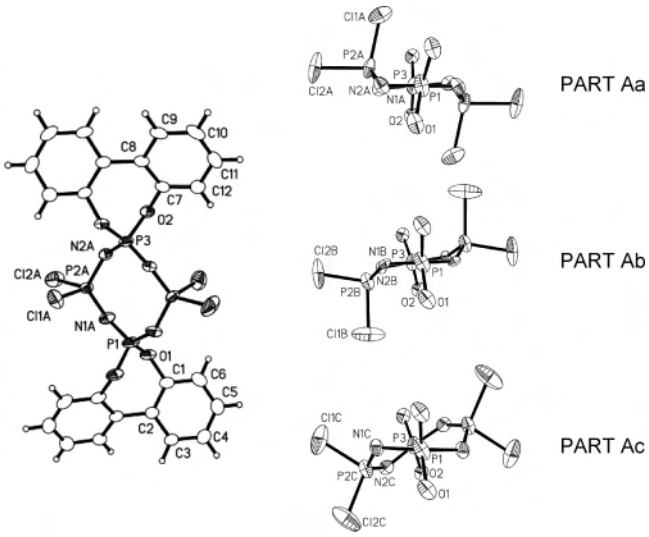

Figure 4. ORTEP representation of *trans*-**2*Aa*** (major disordered form) and a comparison of the three disordered ring conformations (*trans*-**2*Aa*** 53%, *trans*-**2*Ab*** 19%, and *trans*-**2*Ac*** 28%). The thermal ellipsoids are drawn at the 50% probability level.

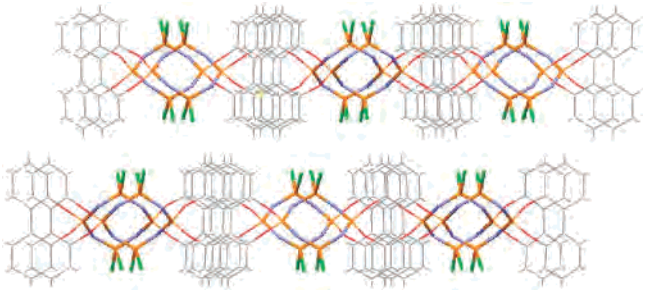

Figure 5. Packing diagram of *trans*-**2*A*** viewed down the *c* axis.

boat form where the ring nitrogen atoms lie alternating above and below a plane defined by the phosphorus centers (Figure 4).

The phosphazene rings are anchored by a rigid set of dioxybiphenyl groups that are π-stacked in columns along the *c* axis (Figure 5). Since the chiral axes of the overlapping dioxybiphenyl moieties have the same configuration, both aromatic rings of each dioxybiphenyl moiety can achieve strong π-overlap with both of the aromatic rings in the dioxybiphenyl moieties of its stacking partners. The mean planes of the overlapping rings in the dioxybiphenyl groups are ~3.57 Å apart and nearly coplanar (the planes are displaced to one another by 0.4°). Thus, the close interlinking of both dioxybiphenyl groups in a molecule with dioxybiphenyl groups on adjacent molecules above and below the mean plane of the phosphazene ring gives rise to two-dimensional sheets of molecules that propagate along the *a* axis. Since R and S configurations of the biphenol group occur at either end of the same molecule, the overall motif within the sheets is an alternating series of columns of R- and S-configured dioxybiphenyl groups, and the displacement of the atoms in the disordered phosphazene ring occurs in a direction roughly parallel with these columns (Figure 6). It has been shown previously for the cyclotriphosphazene analogues that, in solution, rapid interchange of the configurations of the spirocyclic dioxybiphenyl groups is possible[8] and that favorable packing interactions probably govern the occurrence of a particular conformer in the crystalline state[5b,g,8] leading to stereoisomer discrimination.[5g]

In contrast to the orthorhombic structure, the monoclinic structure contains molecules with a well-ordered phosphazene ring conformation (*trans*-**2*B***, Figure 7). Of the four pairs of angles in the phosphazene ring, the angles in the NPN sets are similar [119.29(15) and 123.14(16)°], but the angles in the PNP sets are quite different [131.14(18) and 163.7(2)°]. The four pairs of P−N distances in the ring vary between 1.516(3) and 1.571(3) Å. Consequently, the phosphazene ring has an oval shape, and it is also virtually flat (the mean deviation of the atoms in the ring from the mean plane of the ring is 0.049 Å). The packing interactions of this polymorph are less symmetrical and more varied in nature than those observed in *trans*-**2*A***. Although both the R and S configurations of the biphenol rings are still found on the same molecule, in this case each aromatic ring of a biphenol moiety is involved in $\pi-\pi$ or $\pi-$H interactions with the aromatic rings on two different adjacent molecules. This means that the molecules are involved in π interactions with four neighboring molecules per biphenol rather than two. The sheet-like packing motif of *trans*-**2*A*** is lost as is the opportunity for thermal displacement of the P2 phosphorus atoms, since both bonded chlorine atoms now exhibit close approaches to chlorine or oxygen atoms of the more encroaching adjacent molecules. Specifically, Cl1···Cl1# is 3.411 Å (sum of van der Waals radii is 3.7 Å), and Cl2···O2# is 3.054 Å (sum of the van der Waals radii is 3.25 Å).

The tris-dioxybiphenyl cyclotetraphosphazene compound was obtained in three different crystalline modifications all crystallized from CH_2Cl_2-hexane. Thus **3*A*** (Figure 8a) was obtained as colorless blocks in the triclinic space group $P\bar{1}$ which contained, in addition, two molecules of dichloromethane in the unit cell. On another occasion, the compound again crystallized in the space group $P\bar{1}$ with two dichloromethane molecules but now with two crystallographically independent molecules of **3** (**3*B′*** and **3*B″***) in the asymmetric unit. A third solvent-free crystalline form **3*C*** was observed in the monoclinic space group $P2_1/n$. The structures of **3** exhibit rather puckered phosphazene ring conformations (Figure 8b): the rms deviations of the ring atoms about the least squares are 0.1355, 0.1628, 0.1394, and 0.2014 Å for **3*A***, **3*B′***, **3*B″***, and **3*C***, respectively. In all four molecules, the dioxybiphenyl moieties on opposite sides of the phosphazene ring (subtending P1 and P3 in **3*A***, **3*B′***, or **3*C*** and P5 and P7 in **3*B″***) have opposing conformations, that is, RS or SR, similar to the conformers of *trans*-**2** reported above. Hence the various solid-state forms of **3** observed here have SSR or SRR conformations.

The packing in the two triclinic crystals is virtually identical, and the difference in the unit cells is brought about by the flexibility of the phosphazene ring. Figure 9 shows similar views of the packing in each crystalline form. The figure shows how two distinct ring conformations in **3*B*** (**3*B′***

(8) Amato, M. E.; Carriedo, G. A.; Garcia-Alonso, F. J.; García-Alvarez, J. L.; Lombardo, G. M.; Pappalardo, G. C. *J. Chem. Soc., Dalton Trans.* **2002**, 3047−3053.

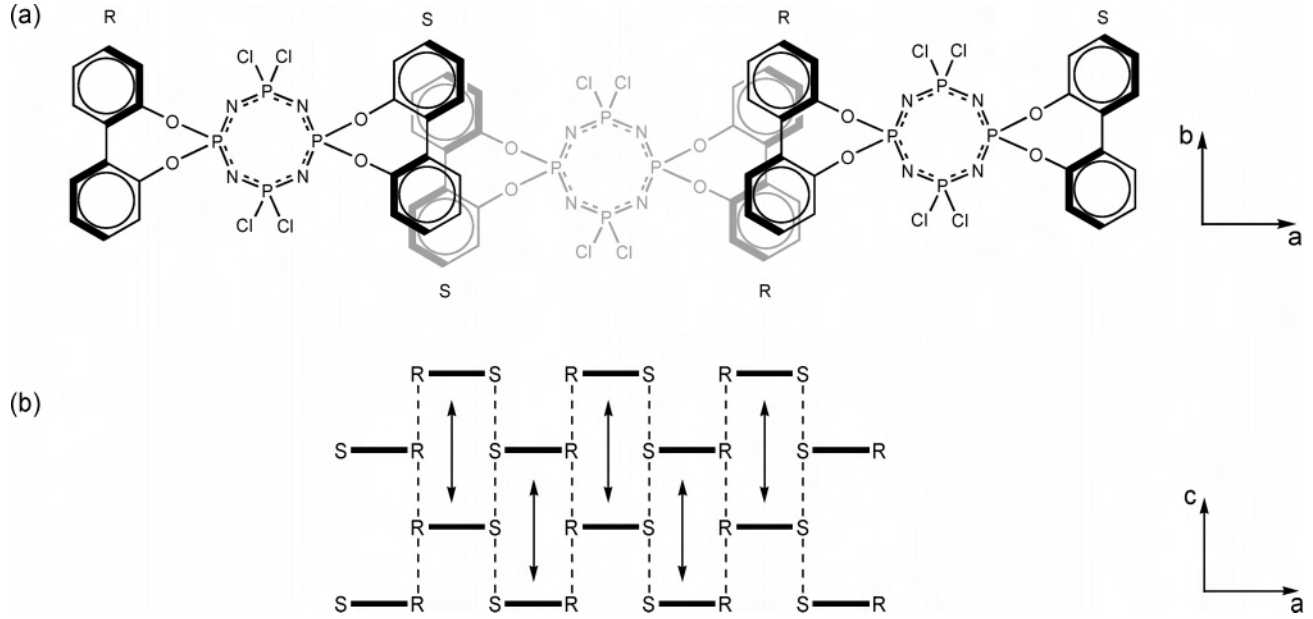

Figure 6. (a) Scheme showing the stacking of dioxybiphenyl rings in *trans*-**2*A***. (b) Cartoon showing the discrimination of stereoisomers in columns along the *c* axis. The double headed arrows in b indicate the space in which the disordered phosphazene ring atoms are displaced.

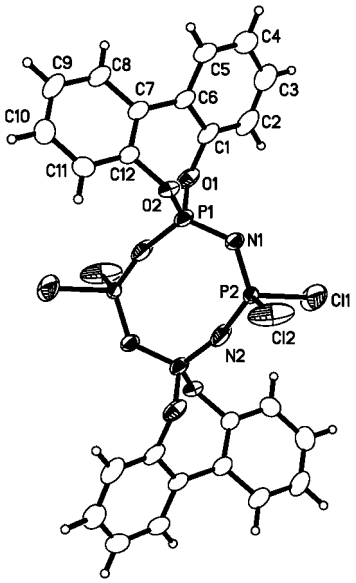

Figure 7. ORTEP representation of *trans*-**2*B***. The thermal ellipsoids are drawn at the 50% probability level.

and **3*B′′***) (Figure 9b) can exist, in comparison to the one conformation observed for **3*A*** (Figure 9a), without significantly changing the packing motif. It should be noted that in **3*A***, atoms N1 and N2 exhibit slightly larger thermal parameters than the other atoms in the phosphazene ring, which may also suggest that further atomic displacement is possible. The data for **3*A*** and **3*B*** were collected at different temperatures [150(2) and 87(2) K] and so the occurrence of the different conformations is probably the result of a phase transition at some point between the two. A similar phenomenon has been reported for the compound $[N_4P_4F_8]$.[9]

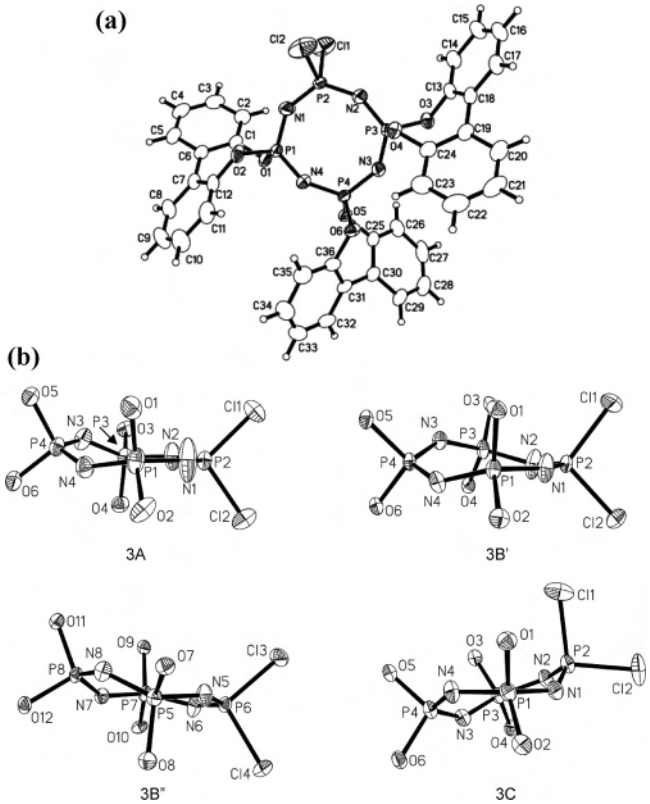

Figure 8. (a) ORTEP representation of **3*A***. The thermal ellipsoids are drawn at the 50% probability level. (b) Comparison of the four phosphazene ring conformations observed in the crystal structures of **3**.

DFT Calculations. To further investigate the structure of *trans*-**2**, DFT calculations on each of the conformations identified from the X-ray diffraction analysis[10] were carried out. The gas-phase structures of both the full system and a model system, where the dioxybiphenyl groups are replaced

(9) Elias, A. J.; Twamley, B.; Haist, R.; Oberhammer, H.; Henkel, G.; Krebs, B.; Lork, E.; Mews, R.; Shreeve, J. M. *J. Am. Chem. Soc.* **2001**, *123*, 10299−10303.

(10) Some of the computed geometeries are the corresponding mirror images of those found in the crystal structures.

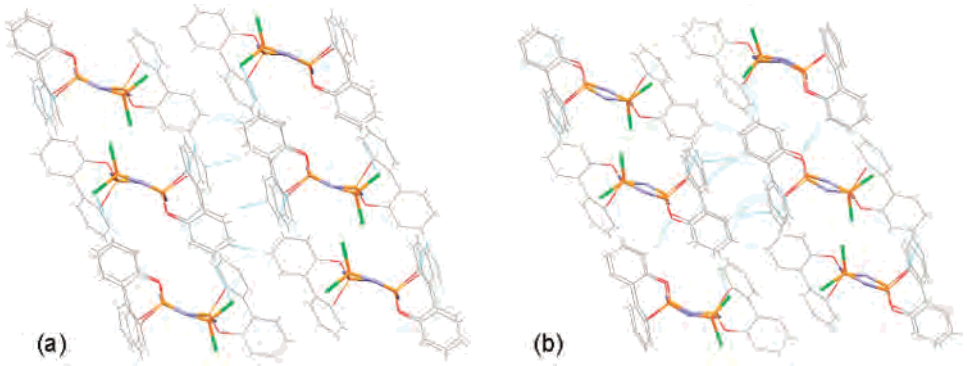

Figure 9. (a) Packing in **3*A*** and (b) **3*B***. The solvent molecules have been removed for clarity.

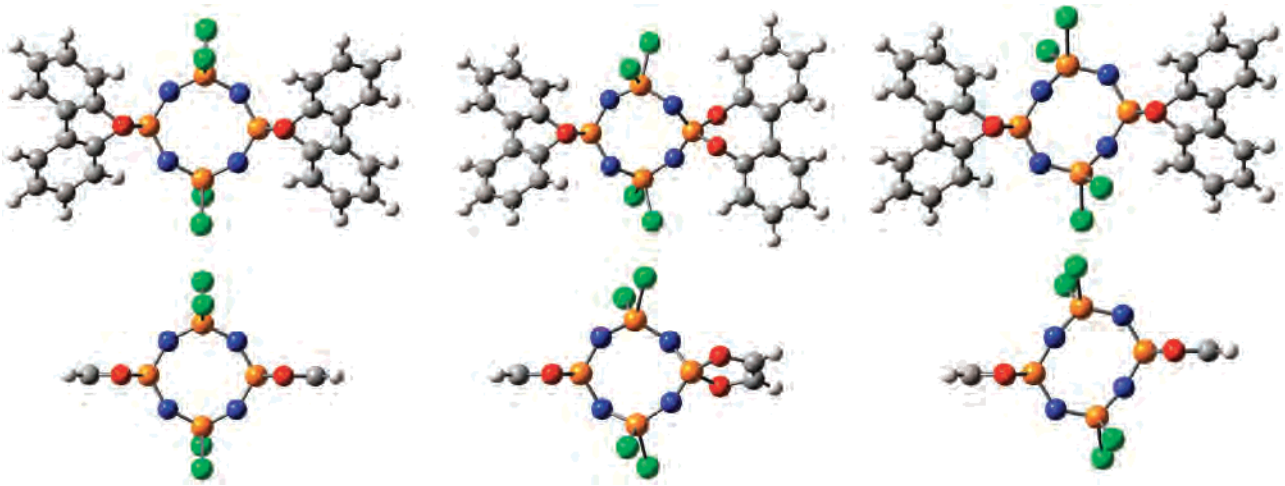

Figure 10. Optimized structures: chair, boat, and oval isomers. Top row: Full structures. Bottom row: Corresponding $O_2C_2H_2$ model structures.

by a model moiety ($O_2C_2H_2$), were used (Figure 10). Agreement between the observed and calculated structural parameters of the oval conformation is generally good (see Table S2 and S3, Supporting Information), although poor for the conformations found in the disordered structure. Notably, in both the full and model calculated boat conformations the opposing exocyclic systems are twisted with respect to each other, with O−P−P−O dihedral angles of −30.1 and −28.3, respectively. Slight twisting is observed experimentally (in the non-disordered portion of the orthorhombic structure), with a O1−P1−P3−O2 dihedral angle of −12.43 (14)°, but absent (by symmetry) in the calculated structures of the chair conformation. There is also a lack of twisting in the oval conformation, although in this case the phosphorus centers are offset because of the deformation of the phosphazene ring. Analysis of the calculated vibrational frequencies confirmed that both the boat and oval conformations are local minima, although the chair conformation is not found to be a local minima; possessing two imaginary frequencies for both the full and model systems. There is, however, a small energy difference between the oval and chair conformations (full system, 3.0 kJ mol^{-1}; model system, 2.3 kJ mol^{-1}) emphasizing the flexible character of the phosphazene ring. From comparison of the crystal packing, the driving force for this conformational change can be attributed to the π stacking of the dioxybiphenyl substituents observed in the orthorhombic structure, but significantly reduced in the triclinic structure. The conformation difference primarily originates from the change in the P−N−P angles from symmetric in the chair conformation (exptl, ∼133°; calcd full, 142.6°; calcd model, 145.6°) to asymmetric in the oval conformation (exptl, 131.1(2)°, 163.7(2)°; calcd full, 131.2°, 151.0°; calcd model, 132.2°, 159.1°), while the N−P−N angles remain unchanged at ∼120°. This observation is in agreement with the general observation that the P−N−P angles are more flexible than that of the N−P−N,[11] and the computed force constants for the N−P−N bend in $ClNPCl_2NCl_2$ (17.5 kJ mol^{-1} rad^{-2}) and the P−N−P bend in Cl_3PNPCl_4 (577 kJ mol^{-1} rad^{-2}).[12]

The observed disorder in the orthorhombic structure was investigated through a relaxed potential energy surface scan of the model system where the $PO_2C_2H_2$ moieties were fixed in place (to model the effect of the π-stacked dioxybiphenyl groups) and the Cl(axial)−P−P−Cl(axial) dihedral angle was varied (Figure 11). The resulting conformation is twisted from the C_{2h} symmetry of the chair form to higher energy, with a corresponding force constant of 75.0 kJ mol^{-1} rad^{-2}. For larger values of the dihedral angle, ∼15−20°, and higher energy, the conformation approaches D_2 symmetry, similar to that of the boat conformation, consistent with the lower occupation of the disorder by *trans*-**2*Ac***. In the case of the

(11) (a) Allcock, H. R. *Phosphorous-Nitrogen Compounds: Cyclic, Linear and High Polymeric Systems*; Academic Press: New York, 1972. (b) Allcock, H. R. *Chem. Rev.* **1972**, *72*, 315−356.
(12) Luaña, V.; Pendás, A. M.; Costales, A.; Carriedo, G. A.; García-Alonso, F. *J. Phys. Chem. A* **2001**, *105*, 5280−5291.

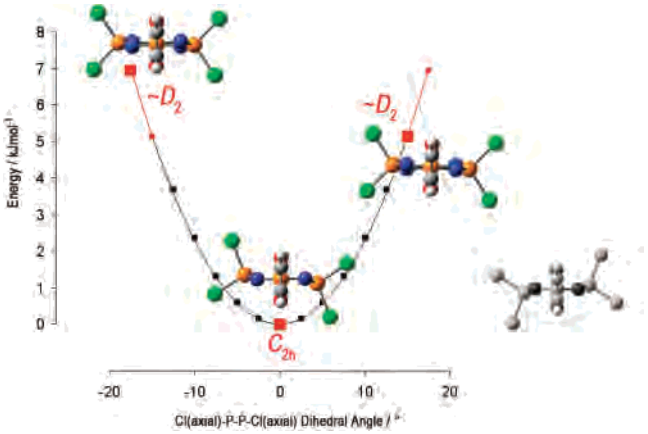

Figure 11. Relaxed potential energy surface (model system) simulating disorder in the orthorhombic structure; generated by fixing the $PO_2C_2H_2$ moieties and varying the Cl(axial)−P−P−Cl(axial) dihedral angle.

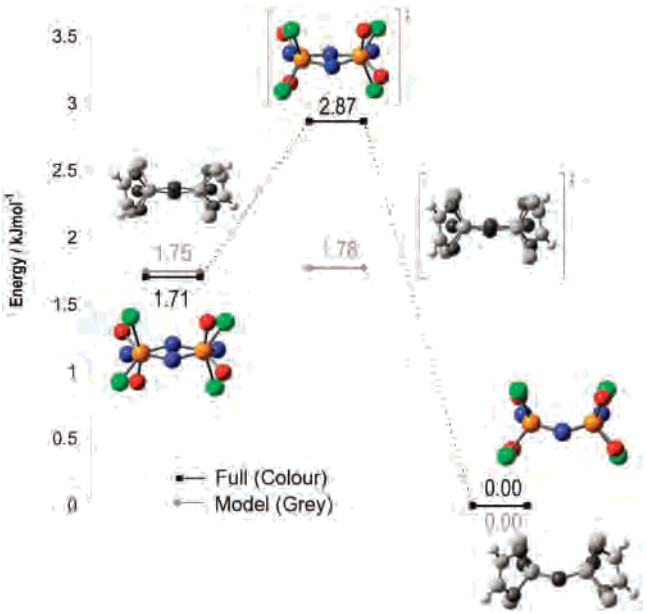

Figure 12. Potential energy diagram for the oval-boat conformation system (dioxybiphenyls omitted for clarity).

dioxybiphenyl-substituted systems, the adoption of this ring conformation could mediate the ring flipping from one chair conformation to another, as depicted pictorially in Figure 11 by the intersection of two potential energy curves, because the resulting directions that the ring may twist back to the chair conformation are inequivalent (as opposed to the model system).

The lowest-energy conformer is found to be the boat conformer: ~1.7 kJ mol^{-1} lower in energy than the oval conformation. A transition state structure connecting the oval and boat conformations was located for both the full and model systems, and the corresponding potential energy diagram is depicted in Figure 12. In the context of the solid-state structures, we conclude that the presence of π-stacking significantly modifies the nature of the potential energy surface and places the energetic importance of this interaction on the order of ~5 kJ mol^{-1} (from the comparison of the conformation energies). A recent bonding analysis of phosphazenes has suggested that the origin of the flexibility in phosphazenes is the largely ionic character of the P−N bond, which is supplemented by smaller π-bonding contributions originating from negative hyperconjugation.[13] These π-bonding interactions appear to build multiple P−N bond character with little hindrance to rotation. Indeed, the computed rotation barrier of the P−N bond in [$HNPCl_3$] (5.9 kJ mol^{-1}) is of similar magnitude to the projected packing energies. Furthermore, in solution, the observed A_2B_2 spin system is indicative of the presence of the more symmetric boat phosphazene ring conformation consistent with the computed energies.

Conclusion

The spiro-substituted derivatives, 2,2′-dioxybiphenyl-hexachlorocyclotetraphosphazene, bis(2,2′-dioxybiphenyl)-tetrachlorocyclotetraphosphazene, and tris(2,2′-dioxybiphenyl)-dichloro-cyclotetraphosphazene have been prepared from the reaction of [$N_4P_4Cl_8$] with 2,2′-biphenol with potassium carbonate as base. The compounds all show non-first-order ^{31}P NMR spectra which were simulated to extract the spectral parameters. Crystals of *trans*-bis(2,2′-dioxybiphenyl)tetrachloro-cyclotetraphosphazene were obtained in orthorhombic (*Pnna*) and monoclinic ($P2_1/n$) space groups. In the orthorhombic structure, the dominant (72%) conformation of one phosphazene ring is a chair, and the other (28%) resembles a boat. For the monoclinic structure, the ring is virtually flat with an oval shape. In both cases, the dioxybiphenyl groups are found in R and S configurations in the same molecule and are π stacked in columns or involved in $\pi-\pi$ or $\pi-$H interactions, thus anchoring the phosphorus atoms of the cyclotetraphosphazenes but still allowing flexibility in the ring conformations. Three crystalline modifications of tris-(2,2′-dioxybiphenyl)dichlorocyclotetraphosphazene were obtained: two with a triclinic ($P\bar{1}$) space group and one with a monoclinic ($P2_1/n$) space group. The cyclophosphazene rings exhibit puckered conformations with the *trans*-dioxybiphenyl moieties having opposing RS or SR conformations. DFT calculations on each of the phosphazene ring conformations in *trans*-bis(2,2′-dioxybiphenyl)tetrachlorocyclotetraphosphazene support the view that intermolecular interactions (i.e., $\pi-\pi$ or $\pi-$H) between the dioxybiphenyl groups are a significant factor in the composition of the overall potential energy surface. The flexibility of the phosphazene ring is supported computationally, through the calculated low-energy barriers, and experimentally, through the highly disordered phosphazene ring conformations observed in the solid state.

The results for 2,2′-dioxybiphenyl-substituted cyclotetraphosphazenes indicate that interactions between the aromatic rings ($\pi-\pi$ or $\pi-$H) will generate microcrystalline domains in 2,2′-dioxybiphenyl-substituted polyphosphazenes which separate regions where the polymer chain is more randomly orientated. The observation that a series of 2,2′-dioxybiphenyl-amine polyphosphazenes has high glass-transition temperatures (T_g = 122 − 150 °C), which increase with increasing 2,2′-dioxybiphenyl substitution,[4b] is consistent

(13) Chaplin, A. B.; Harrison, J. A.; Dyson, P. J. *Inorg. Chem.* **2005**, *44*, 8407−8417.

Table 2. Crystal and Refinement Data for the Compounds *trans*-**2*A***, *trans*-**2*B***, **3*A***, **3*B***, and **3*C***

	trans-**2*A***	*trans*-**2*B***	**3*A***	**3*B***	**3*C***
empirical formula	$C_{24}H_{16}Cl_4N_4O_4P_4$	$C_{24}H_{16}Cl_4N_4O_4P_4$	$C_{37}H_{26}Cl_4N_4O_6P_4$	$C_{37}H_{26}Cl_4N_4O_6P_4$	$C_{37}H_{26}Cl_4N_4O_6P_4$
M	690.09	690.09	888.30	888.30	803.37
T (K)	150(2)	150(2)	150(2)	87(2)	87(2)
cryst syst	orthorhombic	monoclinic	triclinic	triclinic	monoclinic
space group	*Pnna*	$P2_1/n$	$P\bar{1}$	$P\bar{1}$	$P2_1/n$
a (Å)	20.9596(4)	9.8389(5)	11.9325(2)	12.3430(1)	14.2015(2)
b (Å)	18.2750(4)	7.4607(3)	12.3467(2)	15.4971(1)	12.0582(1)
c (Å)	7.5787(2)	19.2015(9)	15.4345(3)	20.7351(3)	20.7909(3)
α (deg)	90	90	69.354(1)	105.069(1)	90
β (deg)	90	99.749(1)	67.676(1)	97.033(1)	95.880(1)
γ (deg)	90	90	68.037(1)	93.288(1)	90
U (Å^3)	2902.92(11)	1389.13(11)	1891.18(6)	3784.53(7)	3451.60(8)
Z	4	2	2	2	4
abs coeff (mm^{-1})	0.668	0.698	0.536	0.535	0.418
reflns measured	15 654	8133	16 352	33 237	30 827
independent reflns	3029 (R_{int} = 0.0200)	2940 (R_{int} = 0.0191)	7120 (R_{int} = 0.0192)	13 739 (R_{int} = 0.0341)	6717 (R_{int} = 0.1006)
final R indices [$I > 2\sigma(I)$]	R1 = 0.0451 wR2 = 0.1131	R1 = 0.0495 wR2 = 0.1007	R1 = 0.0386 wR2 = 0.0870	R1 = 0.0565 wR2 = 0.1179	R1 = 0.0581 wR2 = 0.1116
R indices (all data)	R1 = 0.0512 wR2 = 0.1166	R1 = 0.0595 wR2 = 0.1066	R1 = 0.0505 wR2 = 0.0948	R1 = 0.0835 wR2 = 0.1328	R1 = 0.0990 wR2 = 0.1268

with this. (The fully substituted 2,2′-dioxybiphenyl-homopolymer has an exceptionally high T_g value of 160 °C.)[4a] Evidence that 2,2′-dioxybiphenyl interactions may persist in solution comes from the bimodal nature of the GPC chromatograms of these polymers which have been interpreted in terms of interchain aggregates.[4b] While the 2,2′-dioxybiphenyl interactions in such polymers have not been studied in detail, it should be noted that the excimer fluorescence results strongly suggest the existence of several different types of aromatic ring interactions, including $\pi-\pi$, between aryl side groups in poly(diphenoxy)phosphazene, $[NP(OPh)_2]_n$.[14] In view of the increasing interest in the properties and applications of 2,2′-dioxybiphenyl-substituted polyphosphazenes, more detailed studies on these polymers are warranted.

Experimental Section

General. All synthetic steps were carried out under nitrogen using standard Schlenk techniques. The solvents acetone, dichloromethane, and hexane (Analar) were used as received. Anhydrous K_2CO_3 (BDH) and 2,2′-biphenol (Sigma) were also used as received. Column chromatography was carried out on silica gel 60 from Merck. Microanalyses were performed by the Campbell Microanalytical Laboratory, University of Otago, Dunedin, New Zealand. $^{31}P\{^1H\}$ NMR spectra were recorded on a Bruker Avance 400 spectrometer and were referenced to an external sample of 85% H_3PO_4. For compounds **1**, **2**, and **3**, spectra were simulated using the PERCH software package.[15] Electrospray ionization mass spectra (ESMS) were collected from CH_3CN solutions on a micromass ZMD spectrometer, run in positive-ion mode.

Syntheses of the compounds. (2,2′-Dioxybiphenyl)hexachlorocyclotetraphosphazene (1). A mixture of $[N_4P_4Cl_8]$ (100 mg, 0.22 mmol), 2,2′-biphenol (40.2 mg, 0.22 mmol), and K_2CO_3 (162 mg, 1.1 mmol) in dry acetone (10 mL) was stirred for 15 min at room temperature. The solvent was evaporated in vacuo, and the solid residue was extracted with CH_2Cl_2 (3 × 10 mL) to yield 112 mg (90%) of a white solid containing 3−4% bisubstituted side-product. Recrystallization from CH_2Cl_2−hexane overnight at 4 °C gave the pure product. ^1H NMR ($CDCl_3$): δ 7.561−7.538 (m, 2H), 7.48−7.44 (m, 2H), 7.45−7.37 (m, 2H), 7.34−7.32 (m, 2H). Anal. Calcd for $C_{12}H_8Cl_6N_4O_2P_4$: C, 24.99; H, 1.40; N, 9.71. Found: C, 25.05; H, 1.40; N, 9.70%. ESMS: *m*/*z* 577 $[MH]^+$.

Bis(2,2′-dioxybiphenyl)tetrachlorocyclotriphosphazene (*trans*-2). $[N_4P_4Cl_8]$ (500 mg, 1.08 mmol) and K_2CO_3 (1.491 mg, 10.8 mmol) were added to a stirred solution of 2,2′-biphenol (402 mg, 2.18 mmol) in acetone (12 mL), cooled in an ice bath. After 1 h, the mixture was allowed to warm to room temperature, and it was stirred for another hour. The progress of the reaction was followed by TLC. Evaporation of the solvent in vacuo and extraction with CH_2Cl_2 (3 × 20 mL) yielded 529 mg of a flaky white solid composed of 50% *trans*-**2**, 37% *cis*-**2**, and 10% **3**, shown by ^{31}P NMR. Purification by column chromatography on silica with CH_2Cl_2−hexane (1:1) as the mobile phase allowed the isolation of 400 mg (54%) of a cis/trans mixture of **2**. Fractional recrystallization from CH_2Cl_2−hexane first gave a small portion of NMR-pure trans isomer, and although the later fractions show a concentration of the cis isomer, the pure cis isomer could not be obtained. ^1H NMR ($CDCl_3$): δ 7.57−7.55 (m, 4H), 7.51−7.45 (m, 4H), 7.40−7.36 (m, 8H). Anal. Calcd for $C_{24}H_{16}Cl_4N_4O_4P_4$: C, 41.77; H, 2.34; N, 8.12. Found: C, 42.00; H, 2.47; N, 8.23%. ESMS: *m*/*z* 691 $[MH]^+$.

Tris(2,2′-dioxybiphenyl)dichlorocyclotetraphosphazene (3). $[N_4P_4Cl_8]$ (500 mg, 1.08 mmol) was reacted with 2,2′-biphenol (602 mg, 3.24 mmol) and K_2CO_3 (4.47 mg, 32.4 mmol) in acetone (25 mL) in an ice bath for 1 h, following the procedure described above for **2**. The reaction was monitored by TLC. The ice bath was removed, and the solution was stirred for another hour. After evaporation of the solvent in vacuo, the residue was extracted with CH_2Cl_2 (7 × 10 mL) to yield 885 mg of crude product. Purification by column chromatography yielded 625 mg (72%) of **3**. ^1H NMR ($CDCl_3$): δ 7.53−7.50 (m, 6H), 7.35−7.21 (m, 18H). Anal. Calcd for $C_{36}H_{24}Cl_2N_4O_6P_4 \cdot CH_2Cl_2$: C, 50.03; H, 2.95; N, 6.31. Found: C, 50.08; H, 2.75; N, 6.25%. ESMS: *m*/*z* 803 $[MH]^+$.

Crystallography. Suitable crystals of both *trans*-**2** and **3** were obtained from two different synthetic batches by vapor diffusion of hexane into a CH_2Cl_2 solution. The X-ray data were collected on a Siemens P4 four-circle diffractometer, using a Siemens SMART 1 K CCD area detector. The crystals were mounted in an

(14) (a) Yeung, A. S.; Frank, C. W.; Singler, R. W. *Polymer* **1990**, *31*, 1092−1099. (b) Yeung, A. S., Frank, C. W., Singler, R. W. *Macromolecules* **1991**, *24*, 5539−5545.

(15) Laatikainen, R.; Niemitz, M.; Korhonen, S.-P.; Hassinen, T. *PERCH, An Integrated Software for Analysis of NMR Spectra on a PC*, version 2000; University of Kuopio: Kuopio, Finland, 2000.

inert oil, transferred into the cold gas stream of the detector, and irradiated with graphite-monochromated Mo Kα ($\lambda = 0.71073$ Å) radiation. The data were collected by the SMART program and processed with SAINT to apply Lorentz and polarization corrections to the diffraction spots (integrated 3-dimensionally). Crystal data are given in Table 2. The structures were solved by direct methods and refined using the SHELXTL program.[16] Hydrogen atoms were calculated at ideal positions. Disorder in the solution of *trans*-**2*A*** was satisfactorily modeled by splitting the ring atoms into three parts, depicted in Figure 4, and refined to completeness with occupations of 53, 28, and 19%. Constraints were applied to displacement parameters of the nitrogen and chloride atoms, and atom pairs (P2C and P2C) and (Cl2A and Cl2A) were constrained to share the same coordinates and displacement parameters because of their close proximity from initial refinements.

Computational Details. All geometry optimizations and frequency calculations were carried out using the Gaussian 03 suite of programs,[17] with the exception of the full-system transition state for which the Gaussian 98 suite was used.[18] Density functional theory, using the hybrid B3LYP functional[19] and the 6-31G(d) basis set for all atoms, was used for all geometry optimizations and frequency calculations. A pruned grid consisting of 75 radial shells and 302 angular points was used for the full systems, while a finer grid with 99 radial shells and 590 angular points was used for the model systems. Structures were optimized with appropriate symmetry (chair, C_{2h}; boat, C_2; oval, C_i; transition states, no symmetry).[10] The force constants were calculated at each point for the optimization of the model system structures. The nature of each of the stationary points was determined by vibrational analysis. The boat and oval conformations were found to be local minima for both the full and model systems: a low imaginary frequency (-4 cm^{-1}) for the boat conformation using the full system was found, although we attribute this to residual numerical noise, which is supported by comparison to the model system which has no imaginary frequencies. The chair conformations both possess two imaginary frequencies each: the model system being optimized to a second-order saddle point following the initial optimization and vibrational analysis. Energies are not zero-point corrected. Optimized geometries and data for the relaxed potential energy scan (Table S1) are included in the Supporting Information. Illustrations were created using GaussView 3.0.

Acknowledgment. We acknowledge financial support, including postdoctoral fellowships (to A.D. and C.A.O.), from the Massey University Research Fund and the RSNZ Marsden Fund (MAU208). We thank the New Zealand Foundation for Research, Science and Technology for a Top Achiever Doctoral Fellowship (to A.B.C.) and the Otsuka Chemical Co. Ltd. for a gift of octachlorocyclotetraphosphazene. We are also grateful for access to the Helix parallel-computing facility (Massey University, Auckland) and to Professor G. B. Jameson for helpful advice on the X-ray crystallography.

Supporting Information Available: Crystallographic information for *trans*-**2*A***, *trans*-**2*B***, **3*A***, **3*B***, and **3*D*** in CIF Format, optimized geometries of the different conformations of *trans*-**2**, and Tables S1−S3. This material is available free of charge via the Internet at http://pubs.acs.org.

IC062141T

(16) Sheldrick, G. M. *SHELXL, Suite of Programs for Crystal Structure Analysis*; Institüt für Anorganische Chemie der Universität: Göttingen, Germany, 1998.

(17) Frisch, M. J.; Trucks, G. W.; Schlegel, H. B.; Scuseria, G. E.; Robb, M. A.; Cheeseman, J. R.; Montgomery, J. A., Jr.; Vreven, T.; Kudin, K. N.; Burant, J. C.; Millam, J. M.; Iyengar, S. S.; Tomasi, J.; Barone, V.; Mennucci, B.; Cossi, M.; Scalmani, G.; Rega, N.; Petersson, G. A.; Nakatsuji, H.; Hada, M.; Ehara, M.; Toyota, K.; Fukuda, R.; Hasegawa, J.; Ishida, M.; Nakajima, T.; Honda, Y.; Kitao, O.; Nakai, H.; Klene, M.; Li, X.; Knox, J. E.; Hratchian, H. P.; Cross, J. B.; Bakken, V.; Adamo, C.; Jaramillo, J.; Gomperts, R.; Stratmann, R. E.; Yazyev, O.; Austin, A. J.; Cammi, R.; Pomelli, C.; Ochterski, J. W.; Ayala, P. Y.; Morokuma, K.; Voth, G. A.; Salvador, P.; Dannenberg, J. J.; Zakrzewski, V. G.; Dapprich, S.; Daniels, A. D.;. Strain, M. C; Farkas, O.; Malick, D. K.; Rabuck, A. D.; Raghavachari, K.; Foresman, J. B.; Ortiz, J. V.; Cui, Q.; Baboul, A. G.; Clifford, S.; Cioslowski, J.; Stefanov, B. B.; Liu, G.; Liashenko, A.; Piskorz, P.; Komaromi, I.; Martin, R. L.; Fox, D. J.; Keith, T.; Al-Laham, M. A.; Peng, C. Y.; Nanayakkara, A.; Challacombe, M.; Gill, P. M. W.; Johnson, B.; Chen, W.; Wong, M. W.; Gonzalez, C.; Pople, J. A. *Gaussian 03*, revision D.01; Gaussian, Inc.: Wallingford, CT, 2004.

(18) Frisch, M. J.; Trucks, G. W.; Schlegel, H. B.; Scuseria, G. E.; Robb, M. A.; Cheeseman, J. R.; Zakrzewski, V. G.; Montgomery, J. A., Jr.; Stratmann, R. E.; Burant, J. C.; Dapprich, S.; Millam, J. M.; Daniels, A. D.; Kudin, K. N.; Strain, M. C.; Farkas, O.; Tomasi, J.; Barone, V.; Cossi, M.; Cammi, R.; Mennucci, B.; Pomelli, C.; Adamo, C.; Clifford, S.; Ochterski, J.; Petersson, G. A.; Ayala, P. Y.; Cui, Q.; Morokuma, K.; Malick, D. K.; Rabuck, A. D.; Raghavachari, K.; Foresman, J. B.; Cioslowski, J.; Ortiz, J. V.; Stefanov, B. B.; Liu, G.; Liashenko, A.; Piskorz, P.; Komaromi, I.; Gomperts, R.; Martin, R. L.; Fox, D. J.; Keith, T.; Al-Laham, M. A.; Peng, C. Y.; Nanayakkara, A.; Gonzalez, C.; Challacombe, M.; Gill, P. M. W.; Johnson, B. G.; Chen, W.; Wong, M. W.; Andres, J. L.; Head-Gordon, M.; Replogle, E. S.; Pople, J. A. *Gaussian* 98, revision A.11.4; Gaussian, Inc.: Pittsburgh, PA, 1998.

(19) (a) Becke, A. D. *Phys. Rev. A* **1988**, *38*, 3098−3100. (b) Becke, A. D. *J. Chem. Phys.* **1993**, *98*, 5648−5652.